Synthesis and characterization of thermosensitive hydrogel with improved mechanical properties

Hengjun Gai and Jie Wu
State Key Laboratory Base of Eco-chemical Engineering, College of Chemistry and Molecular Engineering, Qingdao University of Science and Technology, Qingdao 266042, People's Republic of China

Chenyu Wu
College of Materials Science and Engineering, Chongqing University, Chongqing 400044, People's Republic of China

Xuejiao Sun, Fengjun Jia, and Yueqin Yu[a)]
State Key Laboratory Base of Eco-chemical Engineering, College of Chemistry and Molecular Engineering, Qingdao University of Science and Technology, Qingdao 266042, People's Republic of China

(Received 2 May 2015; accepted 22 July 2015)

Semi-interpenetrating polymer network (semi-IPN) and fully interpenetrating polymer network (full-IPN) hydrogels composed of sodium alginate (SA) and *N*-isopropylacrylamide (NIPAAm) were prepared with Ca^{2+} and *N*,*N*′-methylenebisacrylamide (BIS) as the cross-linkers, respectively. The influence of the SA content and crosslinking degree of alginate on thermosensitive, swelling, mechanical, morphological, and thermal properties was investigated in detail. The hydrogels obtained exhibited obvious thermosensitivity and rapid swelling rate. The presence of Ca^{2+} contributed to the improvement of mechanical properties obviously, without altering the thermosensitivity and network porosity of the hydrogels significantly. The compressive strength of full-IPN hydrogel was improved considerably, while the tensile strength was increased by 308.5% than semi-IPN hydrogel. The T_g of full-IPN dried hydrogel ran up to 142.9 °C with respect to 97.3 °C of pure PNIPAAm, and the improvement indicated that hydrogel with more compact structure was prepared.

I. INTRODUCTION

Smart hydrogels which have the capability to undergo significant volume changes in response to small modification of environmental stimulus, such as temperature, pH, solvent composition, or ionic strength, have attracted a great deal of interest recently.[1–5] These hydrogels have been extensively investigated for a variety of biomedical applications, such as controlled drug delivery, tissue engineering, and bioseparation.[6,7] Among smart materials, pH- and temperature-responsive polymeric hydrogels have been extensively studied because these two factors are important for human body. Poly(*N*-isopropylacrylamide) (PNIPAAm) is a well-known member of the thermo-responsive polymer family, exhibiting abrupt phase transition in aqueous solutions at a lower critical solution temperature (LCST) of approximately 32 °C, which is close to human body temperature.[8,9] PNIPAAm chains hydrate to form expanded structures in water when the solution temperature is below its LCST but form compact structures by dehydration when heated to temperature above the LCST.[3] This hydrophilic–hydrophobic transition has been widely studied. In spite of the unique behavior, the poor mechanical property, biocompatibility, and biodegradability of PNIPAAm hydrogel are the main limitation for its biomedical application. In our previous work,[10–12] we dedicated to solving these problems effectively by adding biocompatible and biodegradable materials in hydrogels. In the past decade, they developed various biodegradable materials as cross-linkers applied in synthesis of hydrogels, which gave rise to the improvement of the biocompatibility and biodegradability of hydrogel obviously. The purpose of this study was to solve another limitation-developing the mechanical property of the hydrogel by means of the preparation of interpenetrating networks (IPN), while keeping its thermosensitivity and biocompatibility.

In this article, sodium alginate (SA) was incorporated into the PNIPAAm backbone to keep the biocompatibility and biodegradability of the hydrogel. SA is a biocompatible, natural polymer with pH-sensitive gel-forming ability. It has been used as a matrix for the entrapment and delivery of drugs, which benefits its dissolution and biodegradation under normal physiological conditions.[7] Carboxylic acid groups of the alginate play an important role of ionic interaction with divalent ions such as Ca^{2+}, Ba^{2+} leading to a three-dimensional network.[13] In this

Contributing Editor: Linda S. Schadler
[a)]Address all correspondence to this author.
e-mail: qustyu@163.com
DOI: 10.1557/jmr.2015.233

 © Materials Research Society 2015

https://doi.org/10.1557/jmr.2015.233 Published online by Cambridge University Press

study, we used the method by Nunamaker et al.[14] Poorly soluble calcium ions in the form of $CaCO_3$ are homogeneously mixed with SA and then the Ca^{2+} is solubilized by the addition of D-glucono-δ-lactone (GDL). GDL slowly acidifies the solution, driving the release of Ca^{2+}. Calcium ions bind to the nearest available carboxyl groups on the alginate molecules, crosslinking the hydrogel in a spatially uniform manner.

There are a number of reports referring to SA in combination with crosslinked PNIPAAm to the formation of semi-interpenetrating polymer network (semi-IPN) hydrogels,[15–17] as well as to fully interpenetrating polymer network (full-IPN) hydrogels containing crosslinked PNIPAAm and Ca-alginate.[18,19] The major part of the published studies characterizes the swelling and drug delivery of the hydrogel with respect to pure PNIPAAm hydrogel, without showing the influence on mechanical properties. Here, IPN hydrogel consisting of Ca-alginate and PNIPAAm is prepared to improve the mechanical properties significantly with respect to pure PNIPAAm and semi-IPN hydrogels.

In our study, synthesis and detailed characterization of semi-IPN and full-IPN hydrogels composed of SA and NIPAAm were conducted to investigate the influence of SA and Ca^{2+} content on thermosensitivity, swelling, mechanical property, and morphology. We underlined the advantages of full-IPN hydrogel over semi-IPN and pure PNIPAAm hydrogels. It is possible to synthesize Ca-alginate/PNIPAAm full-IPN hydrogel with improved mechanical property without altering the thermosensitivity, high swelling ratio (SR) and porous structure, which could be very important for the application of thermosensitive hydrogels as drug delivery matrices.

II. EXPERIMENTAL SECTIONS

A. Materials

N-isopropylacrylamide (NIPAAm, Tokyo Kaset Kogyo Co. Ltd.), SA (Qingdao Bright Moon Seaweed Group), *N*,*N*′-methylenebisacrylamide (BIS), *N*,*N*,*N*′,*N*′-tetramethylethylenediamine (TEMED, analytic ultrapure grade), ammonium persulfate (APS, analytic ultrapure grade), Calcium carbonate ($CaCO_3$), GDL. All materials except NIPAAm and SA were purchased from Shanghai Fine Chemical Co. Ltd., China, without further purification.

B. Synthesis of SA/PNIPAAm semi-IPN hydrogels

A series of SA/PNIPAAm semi-IPN hydrogels with different monomer ratios were prepared with BIS as cross-linker by redox polymerization in the presence of APS as initiator and TEMED as accelerator in aqueous media. Briefly, an aqueous solution was prepared by dissolving 1.5 g of NIPAAm and distinct amount of SA (weight ratio of NIPAAm/SA = 100/0, 98/2, 94/6, 90/10, 85/15) and 0.03 g of BIS in 20 mL deionized water. The solution was slowly stirred (to avoid the formation of air droplets), until homogeneous and transparent solution occurred. After bubbling nitrogen for about 20 min, 0.3 mL 6% (mass fraction) APS and 0.2 mL TEMED were added. The mixture was stirred vigorously for 30 s and the polymerization was conducted at room temperature for 24 h. Following the polymerization, the hydrogel was washed three times for 20 min each in excess distilled water to remove the unreacted compounds, and freeze-dried.

C. Synthesis of Ca-alginate/PNIPAAm full-IPN hydrogels

Structurally homogeneous Ca-alginate/PNIPAAm full-IPN hydrogels were made as previously described. As shown in Fig. 1, a series of full-IPN hydrogels with PNIPAA/SA weight ratio of 94/6 were prepared with different amount of Ca^{2+} (calculated in $CaCO_3$) as the cross-linker of alginate. At first, SA, NIPAAm, and BIS were dissolved in distilled water and mixed with $CaCO_3$ to form a suspension. A fresh aqueous GDL solution was then added to the suspension and vortexed to initiate gelation. The $CaCO_3$/GDL molar ratio was set at 0.5 to yield a neutral pH value. 24 h later, APS and TEMED were added. The mixture was stirred vigorously for 30 s and the polymerization was conducted at room temperature for 24 h. Afterward, the full-IPN hydrogels were washed in distilled water to remove the unreacted Ca^{2+}. The morphology of freeze-dried semi-IPN and full-IPN hydrogels was investigated by a scanning electron microscope (JSM-7500F, JEOL, Tokyo, Japan).

D. Measurements of LCST

The LCST of semi-IPN and full-IPN hydrogels was determined by the measurement of their transmittance. Before the measurement, all samples were immersed in distilled water at room temperature and allowed to swell for at least 24 h to reach an equilibrium state. The changes in transmittance of the hydrogels with temperature were captured using an UV–Vis spectrophotometer (λ = 569 nm, path length = 3 cm, Spectrum 723p, Shanghai Spectrum Instruments CO., LTD., China) attached to a high constant temperature bath (CH-1015, Shanghai Precision Scientific Instrument CO., LTD., China). Distilled water was used to calibrate the spectrophotometer. The LCST of the hydrogel sample was determined as the abscissa of the inflection point of the transmittance versus temperature curves.

E. Measurement of swelling kinetics

The swollen hydrogel samples were first lyophilized using a freeze-drying system for 24 h to obtain dehydrated porous xerogels. The swelling behavior of the

https://doi.org/10.1557/jmr.2015.233 Published online by Cambridge University Press

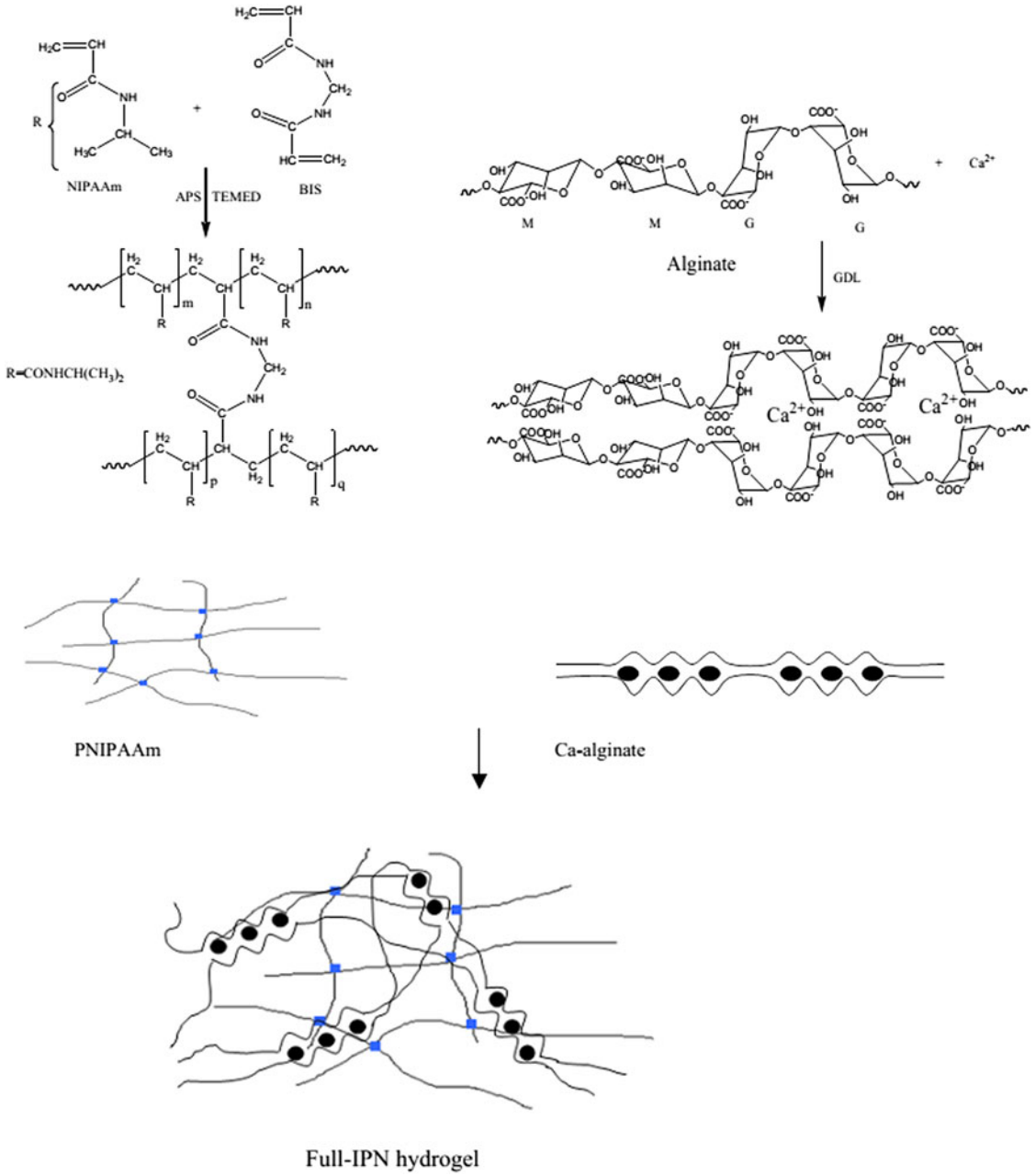


FIG. 1. Schematic structure of the Ca-alginate/PNIPAAm full-IPN hydrogel.

hydrogels was determined by immersing preweighed dried samples to swell in distilled water at 25 °C. At regular time intervals, the swelling hydrogels were taken out to weigh after the removal of the surface water through blotting with filter paper and then put back into the same vials. SR of the sample was calculated according to the following expression:

$$\mathrm{SR} = (W_t - W_d)/W_d \quad , \qquad (1)$$

where W_t is the weight of the wet hydrogel at regular time intervals and W_d is the weight of the dry hydrogel.

F. Measurement of mechanical properties

1. Compression

The mechanical properties of the semi-IPN and full-IPN hydrogels were measured by compressive testing in a TA.XTPlus texture analyzer (Stable Micro Systems, Godalming, UK) using P/0.5 as the analytical probe. The hydrogel, in the form of a cylinder, was placed under the probe, and the test was started. The hydrogel was compressed up to 80% of its original height using a test speed of 1.0 mm/s with a 5 g auto-triggering force. The gel hardness was derived from maximum induction force (g) during the experiment.

https://doi.org/10.1557/jmr.2015.233 Published online by Cambridge University Press

2. Tension

Tension experiments were performed using electronic universal testing machine (Model MZ-4000D, Jiangsu Mingzhu Testing Machine, Yangzhou City, Jiangsu Province, China). For the tensile test, samples of 1.4–1.8 mm in thickness were cut into a dumbbell shape (width of 4 mm, length of 20 mm). Tensile velocity was 300 mm/min. Tensile strength (TS) and elongation (E) at break were obtained during the experiment. TS was expressed in MPa and calculated by dividing the maximum load (N) by the initial cross-sectional area (m^2) of specimen. E was measured using $E = (l_{max} - l)/l$, where l is the initial length, and l_{max} is the change in length at the maximum load.

G. Differential scanning calorimetry (DSC) analysis

Determination of the glass transition temperatures (T_g) of the dried hydrogels were investigated by DSC (204, Netzsch, Selb, Germany). All samples were primarily heated from room temperature to 160 °C at 20 °C min^{-1} under a nitrogen atmosphere for the removal of any residual moisture. Immediately, the samples were cooled to room temperature, and this was followed by reheating to 180 °C at 10 °C min^{-1}. All scans were carried out under a 20 mL min^{-1} flow of nitrogen to prevent oxidation. The T_g was determined as the inflection point of the endothermic drift in the second heating curve of thermogram.

IV. RESULTS AND DISCUSSION

A. Synthesis of semi-IPN and full-IPN hydrogels

NIPAAm was polymerized by radical polymerization with BIS as cross-linker in the presence of APS/TEMED redox reaction system. SA was incorporated into PNIPAAm backbone to prepare semi-IPN hydrogel. Figure 1 showed the schematic structure of full-IPN hydrogels with various compositions of SA and NIPAAm, which were crosslinked with Ca^{2+} and BIS, respectively. The linear hydrophilic SA chains were entrapped in PNIPAAm network and may have some unreacted carboxyl groups available, which were crosslinked with divalent calcium ions partly, forming a full-IPN network Ca-alginate/NIPAAm. The hydrogels, just after preparation, were found to be transparent and elastic, while the dried gels were white and porous. In the present work, we also observed that the transparency of the gels decreased with increasing the SA content or the concentration of Ca^{2+}. Table I summarized the condition of synthesis.

As seen in Fig. 2, the freeze-dried semi-IPN and full-IPN hydrogels presented homogeneous porous structure clearly from the SEM micrographs. And the Ca-alginate/PNIPAAm hydrogel exhibited a similar morphology to semi-IPN hydrogel, which indicated the impact of Ca^{2+} to the morphology of the samples was negligible.

B. Characterization of the LCST

The LCST of the temperature-sensitive semi-IPN and full-IPN hydrogels is the consequence of hydrophobic groups (associated with the isopropyl groups) and hydrophilic groups (associated with the amide groups) interactions in an aqueous environment. The effect of temperature on the transmittance of visible light (λ = 569 nm) through the SA/PNIPAAm semi-IPN hydrogels is shown in Fig. 3. Each line represented a single experiment with one hydrogel sample. Figure 3 showed that all the SA/PNIPAAm semi-IPN hydrogels with different amount of SA had phase transition significantly. In comparison with pure PNIPAAm hydrogel, formation of the semi-IPN structures based on different SA content had not resulted in change of the LCST, which was maintained at about 33 °C. This indicated that there was no chemical bond or other strong interaction between SA and PNIPAAm, while the main driving force of phase transition was the interaction of the hydrophobic and hydrophilic groups in the PNIPAAm backbone. Therefore, the LCSTs of the SA/PNIPAAm semi-IPN hydrogel unchanged. In the whole gel system, the PNIPAAm maintained its independence, which was the characteristic of semi-IPN structure.

The LCSTs of full-IPN obtained by the transmittance versus temperature curves in Fig. 4 showed that all full-IPN samples exhibit the LCST values around 34 °C, near to the body temperature, the volume phase transition temperature was influenced by the presence of Ca^{2+} as the cross-linker of alginate obviously. As seen in Fig. 4, the LCSTs of full-IPN samples with the same weight ratio of NIPAAm/SA (94/6) increased with the addition of Ca^{2+}. However, the full-IPN hydrogels remained obvious thermosensitivity, which was important for the application of it. SA was crosslinked with Ca^{2+} ions easily, which made itself entangled with PNIPAAm network more tightly. Therefore, the motion of PNIPAAm chains requires greater energy for driving hydrophilic–hydrophobic transition, and hence it should result in higher LCST. On the other hand, the temperature response rate gradually slowed down with the increase of Ca^{2+} feeding amount. This is due to the increase in the physical crosslinking density of the hydrogel system, and the structure is more compact and dense. Furthermore, the increase in number of hydrogen bonds between hydroxyl groups in alginate chains and rink-amide groups in PNIPAAm led to the form of a dense hydrophobic layer on the surface of the gel. When the temperature was gradually rising, the speed of water out of the gel was correspondingly slow. So the sensitivity to LCST was obviously decreased with increasing Ca^{2+} feeding amount.

https://doi.org/10.1557/jmr.2015.233 Published online by Cambridge University Press

TABLE I. Composition and mechanical properties of prepared hydrogels.

Samples[a]	Hydrogel	SA (g)	$CaCO_3$/SA (wt%)	Hardness[b] (g)	TS[c] (MPa)	E[c] (%)
1	100/0	0	...	54.440	...	...
2	98/2	0.0300	...	32.106	...	...
3	94/6	0.0957	...	57.017	...	...
4	90/10	0.1667	...	66.247	...	...
5	85/15	0.2647	...	88.478	1.53	397.9
6	85/15	0.2647	2.34	118.723	3.47	285.7
7	85/15	0.2647	4.67	136.254	5.13	228.6
8	85/15	0.2647	7.02	161.077	5.92	232.4
9	85/15	0.2647	9.36	161.820	6.14	263.0
10	85/15	0.2647	18.72	160.327	6.25	234.9
11	85/15	0.2647	28.02	131.179	5.72	207.5

NIPAAm, 1.5 g; BIS, 0.03 g
[a]Samples included pure PNIPAAm (1), semi-IPN hydrogels (2–5), and full-IPN hydrogels (6–11).
[b]Hardness was measured in compression section.
[c]TS and E were measured in tension section.

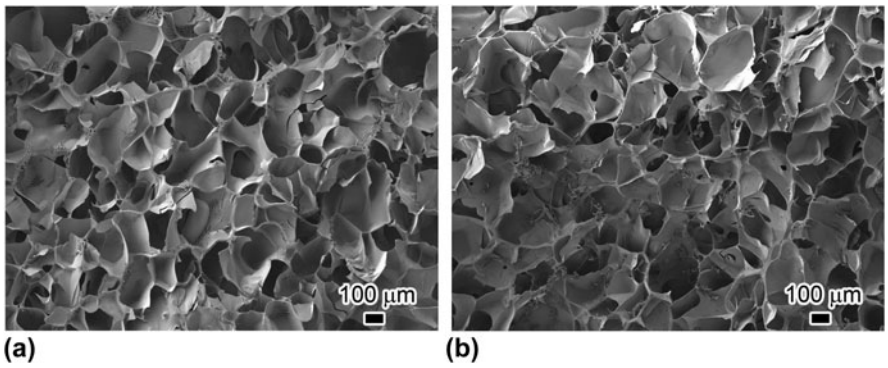


FIG. 2. (a) The fracture SEM micrographs of semi-IPN and (b) full-IPN hydrogels.

C. Measurement of swelling kinetics

Figure 5 showed the swelling kinetics of the dried semi-IPN hydrogel samples with different NIPAAm/SA weight ratios 100/0, 98/2, 94/6, 90/10, 85/15 in distilled water. As seen in Fig. 5, all the dried hydrogels exhibited fast swelling kinetics. The rates of swelling were high during the first 200 min and then gradually decreased until the equilibrium swelling was reached. All samples reached the swelling equilibrium within 750 min. The porous structure of hydrogel (in Fig. 2) might contribute to the fast SR. The diffusion of water molecules into the dry hydrogel was fast at the beginning of the process, which was because the difference of osmotic pressure between the water and the swelling samples was highest initially and it decreased with the expansion of the hydrogel network. Besides, when reaching the swelling equilibrium, the water content increased with increasing hydrophilic monomer SA, which can be attributed to the increased number of free carboxylic acid groups in ionized alginate, which can break hydrogen bonding and generate electrostatic repulsion among alginate macromolecules attracting more water into the hydrogel.

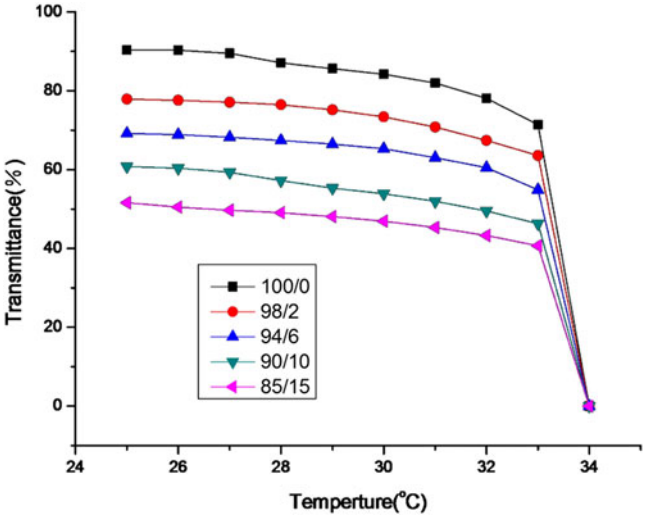


FIG. 3. Transmittance as a function of temperature for SA/PNIPAAm semi-IPN hydrogels with different SA contents.

The swelling kinetics of the full-IPN hydrogels are shown in Fig. 6. From the comparison of two kinds of hydrogel, it could be seen that the SRs of full-IPN

https://doi.org/10.1557/jmr.2015.233 Published online by Cambridge University Press

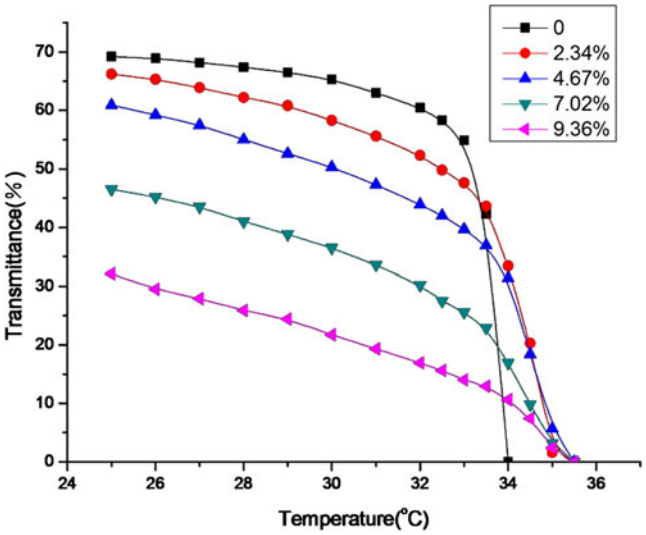


FIG. 4. Transmittance as a function of temperature for Ca-alginate/PNIPAAm full-IPN hydrogels with different Ca^{2+} content, the weight ratio of NIPAAm/SA keeps 94/6.

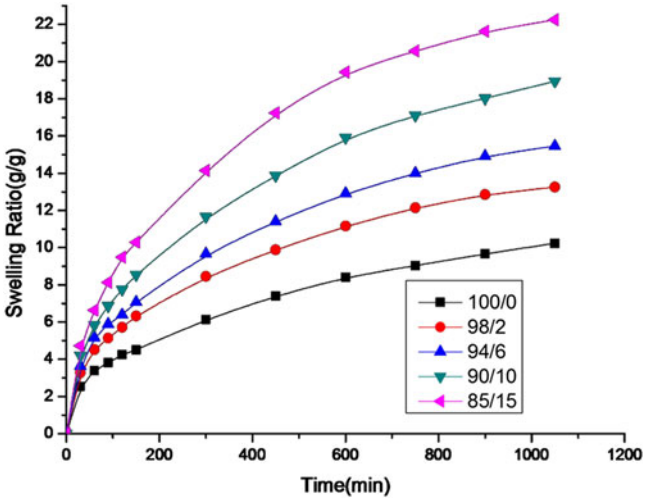


FIG. 5. Effect of the amount of SA in the SA/PNIPAAm semi-IPN hydrogel on the swelling kinetics at 25 °C in distilled water.

hydrogels are lower than semi-IPN hydrogel slightly, which could be explained by that the addition of Ca^{2+} gave rise to the increase of crosslinking density of overall hydrogel, and the more compact structure hindered the inflow of water molecule. Besides, it also could be seen that the SRs of full-IPN hydrogels with different amount of Ca^{2+} (4.67 and 9.36%) were alike, and this indicated that full-IPN hydrogel had fast swelling rate similarly.

D. Measurement of mechanical properties

1. Compression

For effective application of a hydrogel, it is extremely important that the hydrogel presents satisfactory mechanical

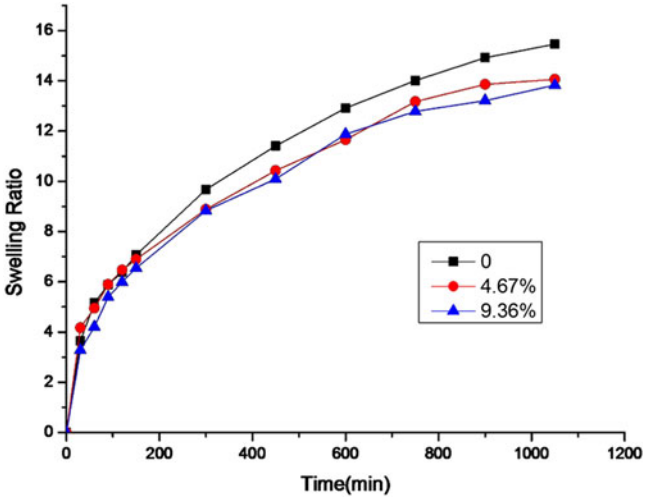


FIG. 6. Effect of Ca^{2+} in the full-IPN hydrogel on the swelling kinetics at 25 °C in distilled water, the weight ratio of NIPAAm/SA keeps 94/6.

properties. The gel hardness for different semi-IPN samples is presented in Table I (samples 1–5). It was found that the addition of a small amount of SA into the hydrogel (98/2) reduced the hardness of the gel in comparison with pure PNIPAAm (100/0), and this could be explained by that the addition of SA hindered the crosslink of NIPAAm chains slightly and decreased the crosslinking density of PNIPAAm network. Besides, the formation of porous structure of semi-IPN hydrogel could also contribute to the decrease of the compressive strength. However, the gel hardness was increasing with the increase in SA concentration in the semi-IPN hydrogels because of the more addition of the liner copolymer SA and PNIPAAm networks were physically entangled with each other more strongly, which increased the physical crosslink density of the hydrogels and made them more compact.

The compressive strength of full-IPN hydrogel (85/15) with different amount of Ca^{2+} as the cross-linker of SA, displayed in Table I (samples 5–11), clearly indicates that the gel hardness was considerably influenced by Ca^{2+} density in the full-IPN samples. An increase of Ca^{2+} concentration in full-IPN hydrogels led to the enhancement of gel hardness obviously. When the Ca^{2+} content reached 7.02% of SA, the gel hardness ran up to the maximum and kept constant. IPNs have two independent polymers forming intertwined networks and are prepared by nonintervening polymerization and crosslinking. In this full-IPN samples, Ca-alginate polymer intertwined with the PNIPAAm network partly, which reduced the mobility of the crosslink points. Moreover, the rest of Ca-alginate polymer filled in the "space" of the PNIPAAm networks, and the hydrogel system dissipated energy through its structural deformation to prevent the emergence of macroscopic cracking. Therefore, an improvement

https://doi.org/10.1557/jmr.2015.233 Published online by Cambridge University Press

in mechanical strength was observed when Ca^{2+} content rises, as a result of the increase in overall chemical and physical crosslinking density of hydrogels. In addition, the gel hardness reduced when the Ca^{2+} content reaches 28.08% because of the extra Ca^{2+} led to the friability of the hydrogels. This phenomenon gave rise to the formation of a more compact and tight network structure, giving improved mechanical properties. According to the results, the hydrogels with good mechanical property could be prepared by controlling the Ca^{2+} content for drug delivery in the next research step.

2. Tension

The result of the tensile property of full-IPN hydrogels with NIPAAm/SA weight ratio 85/15 was presented in Table I. The pure PNIPAAm and semi-IPN hydrogels had not been analyzed because they were too fragile for adequate manipulation, indicating their mechanically weak structure. As shown in Table I, the TS reached their maximum when Ca^{2+}/SA = 18.72%, near to 6.25 MPa, increasing by 308.5% than semi-IPN (85/15) without Ca^{2+}. In fact, when the Ca^{2+} content reached 7.02% of SA, the TS ran up to be higher than semi-IPN hydrogel obviously and kept constant, which was in accordance with the results of compressive test. The results showed that the addition of Ca^{2+} into the hydrogel caused improved mechanical property significantly. This could be explained by that Ca^{2+} crosslinking with carboxylate groups of G unit on the SA chains gave rise to high destiny of overall hydrogel. The high crosslink density enhanced the strength of Ca-alginate network and PNIPAAm network and resulted in a decrease in the flexibility of the full-IPN hydrogel. In contrast, the E of the hydrogel decreased in the presence of Ca^{2+}. From Table I, the E of semi-IPN hydrogel (85/15) was 397.9%, while it decreased to 207.5% of the full-IPN hydrogel. The contrary trend indicated the addition of Ca^{2+} could be able to form a sufficiently crosslinked Ca-alginate network in the hydrogel.

E. DSC analysis

The T_g of the pure PNIPAAm (97.3 °C), semi-IPN (135.5 °C), and full-IPN (142.9 °C) hydrogels were obtained by DSC as it can be seen in Fig. 7. Our study showed that the SA and Ca-alginate considerably contributed to the improved stability of IPNs, in contrast to pure chemically crosslinked PNIPAAm hydrogel. The addition of SA and Ca-alginate resulted in the increase in T_g values, owing to the increase of hydrogen bond of the overall hydrogel and hindering of the chain mobility. Therefore, the formation of IPNs hydrogels led to the improvement in strength of interactions on a molecular level, which was favorable to the application of the hydrogels.

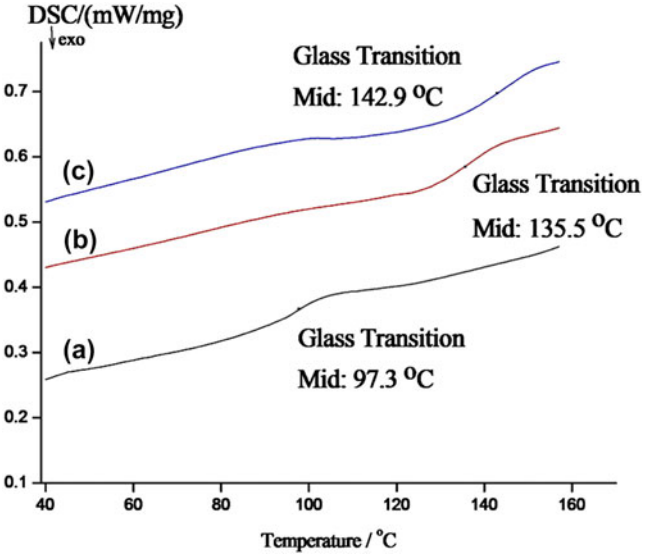


FIG. 7. DSC thermograms for the determination of T_g values of (a) pure PNIPAAm, (b) semi-IPN and (c) full-IPN dried hydrogels.

V. CONCLUSIONS

The work presented in this article dealt with the synthesis and detailed characterization of semi-IPN and full-IPN hydrogels potentially applicable as drug delivery matrices. From the study, it was found that the addition of SA into the PNIPAAm backbone had not impact on the LCST of the hydrogel. The presence of Ca^{2+} in full-IPN hydrogel had no considerable influence on the LCST values (about 34 °C) with respect to semi-IPN hydrogel. The swelling studies showed that increase in SA content significantly improves the swelling rate and equilibrium SR. And the addition of Ca^{2+} had little influence on the swelling. Higher Ca^{2+} content contributed to the improved compressive strength and TS of the full-IPN hydrogels, resulting in a compact and tighter network structure. This was an accordance with the results of the measurement of T_g. The micrographs by SEM showed that the full-IPN hydrogel had the same porous structure with semi-IPN hydrogel.

ACKNOWLEDGMENTS

This research was supported by the National Natural Science Foundation of China (No. 20876081), the National Key Technology Support Program of China (No. 2014BAC10B01), and key scientific and technological project of China's Shanxi Province (No. MN2014-10).

REFERENCES

1. R.P. Dumitriu, G.R. Mitchell, and C. Vasile: Multi-responsive hydrogels based on N-isopropylacrylamide and sodium alginate. *Polym. Int.* **60**(2), 222–233 (2011).
2. K. Kabiri, M.J. Zohuriaan-Mehr, H. Mirzadeh, and M. Kheirabadi: Solvent-, ion- and pH- specific swelling of poly

https://doi.org/10.1557/jmr.2015.233 Published online by Cambridge University Press

(2-acrylamido-2-methylpropane sulfonic acid) superabsorbing gels. *J. Polym. Res.* **17**, 203–212 (2010).
3. H.K. Ju, S.Y. Kim, S.J. Kim, and Y.M. Lee: pH/temperature-responsive semi-IPN hydrogels composed of alginate and poly(N-isopropylacrylamide). *J. Appl. Polym. Sci.* **83**(5), 1128–1139 (2002).
4. D.X. Li, Y. Cui, K.W. Wang, Q. He, X.H. Yan, and J.B. Li: Thermosensitive nanostructures comprising gold nanoparticles grafted with block copolymers. *Adv. Funct. Mater.* **17**, 3134–3140 (2007).
5. D.X. Li, Q. He, Y. Cui, K.W. Wang, X.M. Zhang, and J.B. Li: Thermosensitive copolymer networks modify gold nanoparticles for nanocomposite entrapment. *Chem. Eur. J.* **13**, 2224–2229 (2007).
6. S.P. Zhao, F. Zhou, and L.Y. Li: pH-and temperature-responsive behaviors of hydrogels resulting from the photopolymerization of allylated chitosan and N-isopropylacrylamide, and their drug release profiles. *J. Polym. Res.* **19**(9), 9944 (2012).
7. J. Shi, N.M. Alves, and J.F. Mano: Drug release of pH/temperature-responsive calcium alginate/poly(N-isopropylacrylamide) semi-IPN beads. *Macromol. Biosci.* **6**, 358–363 (2006).
8. I. Asmarandei, G. Fundueanu, M. Cristea, V. Harabagiu, and M. Constantin: Thermo- and pH-sensitive interpenetrating poly(N-isopropylacrylamide)/carboxy-methyl pullulan network for drug delivery. *J. Polym. Res.* **20**, 293–306 (2013).
9. E.C. Cho, J. Lee, and K. Cho: Role of bound water and hydrophobic interaction in phase transition of poly(N-isopropylacrylamide) aqueous solution. *Macromolecules* **36**, 9929–9934 (2003).
10. Y.Q. Yu, Z.Z. Li, H.J. Tian, S.S. Zhang, and P.K. Ouyang: Synthesis and characterization of thermoresponsive hydrogels cross-linked with acryloyloxyethylaminopolysuccinimide. *Colloid Polym. Sci.* **285**, 1553–1560 (2007).
11. Y.Q. Yu, Y. Xu, H.S. Ning, and S.S. Zhang: Swelling behaviors of thermoresponsive hydrogels cross-linked with acryloyloxyethylaminopolysuccinimide. *Colloid Polym. Sci.* **286**, 1165–1171 (2008).
12. Y.Q. Yu, Y.S. Li, L.X. Liu, C.J. Zhu, and Y. Xu: Synthesis and characterization of pH-and thermoresponsive poly(N-isopropylacrylamide-co-itaconic acid) hydrogels crosslinked with N-maleyl chitosan. *J. Polym. Res.* **18**, 283–291 (2011).
13. S. Saha, A. Pal, S. Kundu, S. Basu, and T. Pal: Photochemical green synthesis of calcium-alginate-stabilized Ag and Au nanoparticles and their catalytic application to 4-nitrophenol reduction. *Langmuir* **26**(4), 2885–2893 (2010).
14. E.A. Nunamaker, E.K. Purcell, and D.R. Kipke: In vivo stability and biocompatibility of implanted calcium alginate disks. *J. Biomed. Mater. Res., Part A* **83A**(4), 1128–1137 (2007).
15. R. Hernandez and C. Mijangos: In situ synthesis of magnetic iron oxide nanoparticles in thermally responsive alginate-poly(N-isopropylacrylamide) semi-interpenetrating polymer networks. *Macromol. Rapid Commun.* **30**(3), 176–181 (2009).
16. G.Q. Zhang, L.S. Zha, M.H. Zhou, J.H. Ma, and B.R. Liang: Rapid deswelling of sodium alginate/poly(N-isopropylacrylamide) semi-interpenetrating polymer network hydrogels in response to temperature and pH changes. *Colloid Polym. Sci.* **283**(4), 431–438 (2005).
17. S.B. Lee, E.K. Park, Y.M. Lim, S.K. Cho, S.Y. Kim, Y.M. Lee, and Y.C. Nho: Preparation of alginate/poly(N-isopropylacrylamide) semi-interpenetrating and fully interpenetrating polymer network hydrogels with γ-ray irradiation and their swelling behaviors. *J. Appl. Polym. Sci.* **100**(6), 4439–4446 (2006).
18. M.R. De Moura, F.A. Aouada, S.L. Favaro, E. Radovanovic, A.F. Rubira, and E.C. Muniz: Release of BSA from porous matrices constituted of alginate- Ca^{2+} and PNIPAAm-interpenetrated networks. *Mater. Sci. Eng., C* **29**(8), 2319–2325 (2009).
19. J.F. Piai, M.R. de Moura, A.F. Rubira, and E.C. Muniz: Kinetic study of bovine serum albumin (BSA) released from alginate-Ca^{2+}/PNIPAAm hydrogels. *Macromol. Symp.* **266**(1), 108–113 (2008).

https://doi.org/10.1557/jmr.2015.233 Published online by Cambridge University Press